Intra-day Variability Quantification from Ground-Based Measurements of Global Solar Irradiance

Omaima ElAlani*‡, Hicham Ghennioui *, Abdellatif Ghennioui***

** Laboratory of Signals, Systems and Components, Faculty of Sciences and Technologies: Sidi Mohamed Ben Abdellah University, B.P. 2202 – Route d'Imouzzer, Fes, Maroc.

*** Green Energy Park (IRESEN, UM6P), Route Régionale Kelaa, Km 3 R206, BenGuerir, Maroc.

(omaima94.elalani@gmail.com, hicham.ghennioui@usmba.ac.ma, ghennioui@iresen.org)

‡ Omaima ElAlani; Route Régionale Kelaa 'Km 3 R206, BenGuerir, Maroc, Tel: +212 (0) 6 33 54 12 53, omaima94.elalani@gmail.com.

Received: 02.09.2020 Accepted:02.10.2020

Abstract- Worldwide electricity production has switched from fossil fuel combustion to renewable energy sources and solar power generation has increased significantly in recent years, particularly in the form of photovoltaic (PV) power. Solar radiation is mainly influenced by the process of sunlight interaction with clouds. Being able to quantify the variability of solar irradiance due to clouds is crucial for better integration of the energy generated in the power grid by reducing the uncertainties in solar irradiance forecasts. Our objective is the characterization of a given solar site by quantifying the variability of solar irradiance caused by clouds. To do so, we provide a classification scheme of clouds conditions classes based on the daily clear sky index K_c, and the hourly intraday variability $\delta(K_c)$ defined by the standard deviation of the variations of the clear sky index. As a result of irradiance classification, we obtained nine classes identified as the clear sky (A), mixed (B), and overcast (C) conditions and subdivided into three categories: low (I), medium (II), and high variability (III). We used the solar irradiance data set measured at the high precision meteorological station installed in Benguerir, Morocco, for the period from 01/01/2018 to 31/12/2018. We found that clear sky conditions with low variability (class AI) are the most frequent with a percentage of (38%). Followed by clear sky conditions with medium variability (AII) and mixed sky conditions with medium variability (BII) with a percentage of 18.27% and 19.23% respectively. Other classes are also present with low intensity ranging from 2.5% to 0.95%.

Keywords Solar irradiance, Clear sky, Variability, Photovoltaic.

1. Introduction

Renewable energy sources, such as solar, wind, hydraulic and geothermal energies, currently reflect the future of energy progress, and the market for renewable electricity has experienced a significant acceleration in recent years [1, 2]. The combined share of variable solar and wind power in the energy sector is expected to reach 58% in 2050 [3]. Photovoltaic is one of the most promising renewable energy technologies and the number of PV installations is growing faster than all other renewable energies [4, 5].

However, PV power is an intermittent source of energy, and its production is highly dependent on incident solar irradiance GHI (Global Horizontal Irradiance) [6, 7]. The large-scale penetration of PV installations into the grid is severely limited by the uncontrollable variability of solar irradiance at ground level, which can lead to grid stability problems [8–10]. So, one of the main obstacles to increase the share of PV energy is its intermittency. Since PV generation is highly correlated with incident solar irradiance at ground level, the variability characteristics of solar irradiance will be directly applied to the variability of PV generations [11, 12].

A classification scheme of solar irradiance according to cloud conditions can be useful for different applications of solar energy such as evaluating solar irradiance forecast models under different cloud conditions; which allows reducing the uncertainty in solar irradiance forecasts and enable accurate predictions, allow efficient use of the fluctuating energy production of PV systems, to compare the characteristics of different solar sites and determine the most dominant meteorology, and finally to choose the most

appropriate solar technology for a given site based on the classification results.

Various methods are reported in the literature to quantify the solar irradiance variability, and according to Blaga et al. [13] until now, there is no appropriate method that can be employed for this purpose.

Paulescu and Badescu [14] evaluated the variability of solar irradiance time series by classifying days according to the sunshine stability index, which indicates how many times the sun is covered (or uncovered) by clouds in a time interval.

Perez et al. [15] present an empirical model for quantifying solar irradiance variability for 20 seconds, 1 min, 5 min, and 15 min time scales, based on the clear sky index. As quantifiers of the intra-hourly variability, the standard deviation of the global clear sky irradiance index and the mean variation of the clear sky index between two consecutive time intervals have been used. In our study, this daily clear sky index will be used, but to quantify the intraday variability with a one-hour variability time scale.

Stein et al. [16] proposed a new variability index VI, defined as the ratio of the length L of the measured irradiation as a function of time divided by the length L_{cs} of the clear sky irradiation as a function of time.

Kang and Tam [17] proposed a new method for characterizing and classifying daily sky conditions using the daily clear sky index and a new metric named daily probability of persistence (POPD). The authors found that the proposed method provides interesting results and the different classes obtained are significant for all study sites.

Lave et al. [10] have introduced a new metric called the variability score from the ramp rate distribution to quantify the variability of solar irradiance at a small temporal scale.

Lauret et al. [18] analyzed the intraday variability of irradiance in order to characterize a given location by examining the relationship between two parameters, the daily clear sky index and the intraday variability for 20 sites with various types of climate. They found that the model depends on the site location, hence they proposed two alternative models for sites where cloud formation is influenced by local orography and sites where cloud formation is only traceable to meteorological events.

Schroedter-Homscheidt et al. [8] defined eight classes to characterize the variability of direct normal irradiance (DNI) resolved over 1 minute in one hour, they found that up to 77% of all class members are correctly identified.

In their paper [19], Blaga and Paulescu presented a characterization of the stochastic nature of solar irradiance series from different angles, by analyzing six different quantifiers of solar irradiance variability. To compare these different quantifiers they introduced a new multiparametric ranking procedure to classify days according to the solar irradiation variability model.

Lohmann reviewed in his paper [20] the recent progress in the characterization of solar irradiance variability on small spatial and temporal scales. According to the author, although there are many papers treating the solar irradiance variability issue, there are still a few appropriate high-resolution measurement data to robustly validate the existing models.

Fernandes et al. [21] proposed a methodology to obtain probabilistic models based on probabilistic density functions (PDF) and Clear Sky Index (CSI) to represent the variability of solar irradiation for a given location. To validate the obtained models the authors used two criteria: the Mean Square Error (MSE) and the Chi-Square test.

The aim of this study is to perform an analysis of intraday solar irradiance variability based on previous studies. In order to do this, as a first step, we will characterize the study site based on two criteria: (1) the daily clear sky index K_c, which is used to define the weather conditions of a given day, and (2) the hourly intraday variability measured by the standard deviation of changes in the clear sky index $\delta(K_c)$ [15]. Based on these two indices we have established a classification scheme of cloud conditions classes. We obtained nine classes identified as the overcast, mixed, and clear sky conditions and subdivided into three categories: low, medium, and high variability.

In addition to these two indices, we have determined the corresponding variability for each day, by using the variability index proposed in [16] and defined by the ratio of the GHI length to the GHI length under clear conditions. Finally, we have calculated the sunshine number (SSN) corresponding to each day in order to obtain a better characterization of the study site.

This document is organized as follows: In section 2, we start with a description of the study site and the pyranometric measurements used, followed by a description of the clear-sky solar irradiance and the model used throughout the study. Section 3 focuses on the description of the different solar irradiance quantifiers used to characterize solar variability. In section 4, we evaluate the intraday variability of solar radiation using the different quantifiers described in section 3. In section 5, we discuss the results and provide summaries.

2. STUDY SITE and DATA

2.1. Ground Measurement

To perform this study, we used the one-minute GHI (Global Horizontal Irradiance), DHI (Diffuse Horizontal Irradiance), and DNI (Direct Normal Irradiance) collected from the high-precision meteorological station installed in Benguerir (latitude: 32.12°E, longitude: -7.94°N, altitude: 450 m). GHI and DHI are measured respectively with a Kipp & Zonen CMP11 pyranometer and a Kipp & Zonen CMP11 shading ball pyranometer, while DNI is measured with a Keep & Zonen first class pyrheliometer. Table 1 summarizes the instruments used to measure each irradiance components. The study period is from January 2018 to December 2018, with a temporal resolution of one minute.

A preliminary step is necessary before using data, it consists of:

➢ A quality check of solar data: with any ground measurement, there are errors in the time series of solar data because of sensor problems or because of acquisition issues, so to ensure the good quality of the data a Quality Control algorithm has been applied.

➢ A pre-processing of the data: all night hours are removed, because of problems occurring at sunset and sunrise (masking effects, etc.), and the bad response of the pyranometers) [15] and in addition that the night values do not contain any information. So a filter is applied to keep only the values with SZA (Solar Zenith Angle) < 80°. The SZA per minute has been calculated from the solar geometry SG2 equations [16].

Table 1. Sensors used to measure GHI, DHI and DNI.

Solar irradiance component	Measurement sensor
GHI	Thermopile pyranometer Kipp&Zonen CMP21
DHI	Thermopile pyranometer Kipp&Zonen CMP21 with a shadow-ball (Solys2 sun tracker)
DNI	Pyrheliometer Kipp&Zonen CHP1 (Solys2 sun tracker)

2.2. Solar Irradiance under Clear Sky Conditions

Clear sky irradiance is the solar irradiance under a cloudless sky. This irradiance can be useful to calculate solar indices, to normalize the solar radiation time series, and to obtain the output of solar power plants under stationary conditions [22]. Fig. 1 illustrates the three components of solar irradiance, which are the GHI and GHI_{clear}, the Diffuse Horizontal Irradiance (DHI), and the Beam Horizontal Irradiance (BHI) for both clear and overcast sky conditions. Among the different clear sky models reported in the literature, we have chosen the McClear [23] which is a fast model of surface solar irradiance under cloudless conditions (clear sky), based on the radiative transfer model libRadtran that exploits the clear sky atmospheric optical properties (notably partial and total Aerosol Optical Depths—AOD—at different wavelengths, total contents of water vapor and ozone) provided by the EU-funded Copernicus Atmospheric Monitoring Service (CAMS) [24]. The choice of the model was based on the results of a previous validation of McClear for the same weather station as this study, where satisfactory results were obtained. An RMSE (Root Mean Square Error) of 2.2% and a CC (Correlation Coefficient) of 0.99 for GHI [25].

To quantify the variability caused by clouds, it is required to separate the clouds effect from the deterministic seasonal and diurnal variability of the solar irradiation time series. For this purpose, the clear sky index K_c is calculated (Eq. 1), which is the ratio of the measured solar irradiation GHI to the modeled clear sky irradiation GHI_{clear}.

$$K_c = \frac{GHI}{GHI_{clear}} \tag{1}$$

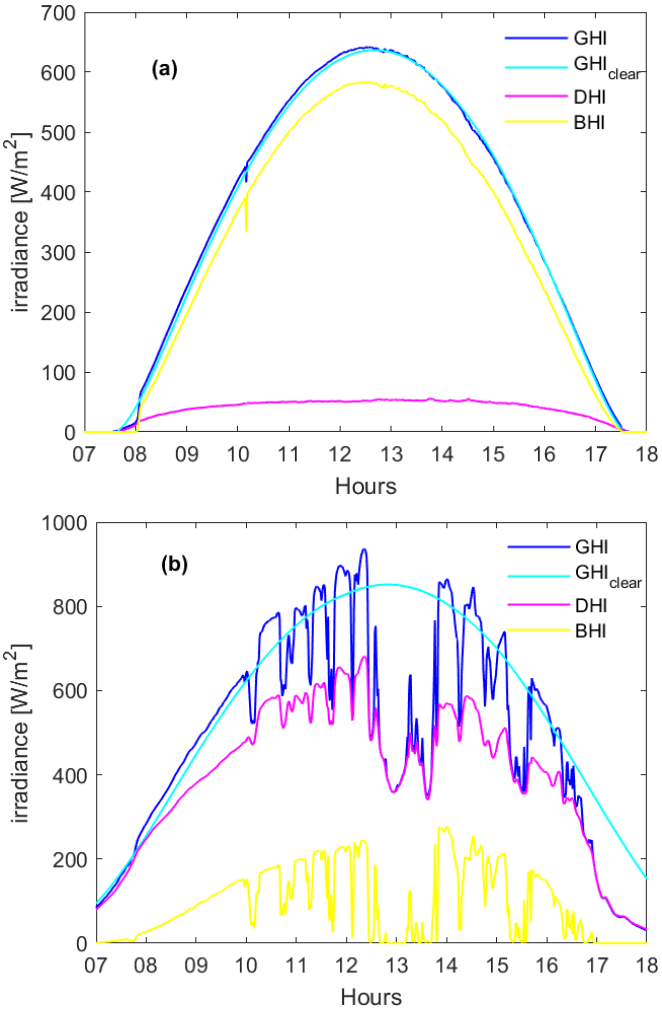

Fig. 1. An example of a diurnal cycle of measured global horizontal irradiation (GHI), diffuse horizontal irradiance (DHI), beam horizontal irradiance (BHI), and clear sky irradiance GHI_{clear} derived from the McClear model. For clear sky (a) and overcast sky (b).

3. Quantifiers for the Solar Irradiance

The solar irradiance variability is mainly caused firstly by the movement of the sun and then by the clouds. The first type of variability is predictable using the solar geometry equations, while the variability due to the movement of clouds is not. This variability can cause irregular fluctuations in the power output of a photovoltaic system.

Three quantities were used to characterize the solar site, which are the daily clear sky index K_c, the daily variability given by the standard deviation of the variation of the clear sky index for the considered day, the irradiance line length, and the sunshine.

3.1. Daily Clear Sky Index

The daily clear sky index K_c is used to characterize the daily solar conditions it is defined by Eq. (2):

$$K_c = \frac{GHI}{GHI_{clear}} \tag{2}$$

$$K_c = \frac{\sum_{n=1}^{N} GHI(n)}{\sum_{n=1}^{N} GHI_{clear}(n)}, \tag{3}$$

where N is the number of daylight hours.

3.2. Hourly Intraday Variability

Different methods exist to quantify solar irradiation variability time series. In our study we used the method proposed by [26] who defines the variability index $\delta(K_c)$ as the standard deviation of the temporal differences of K_c in a time interval Δt.

$$\delta(K_c) = \sqrt{\frac{1}{N}\sum_{n=1}^{N}(\Delta K_c)} \tag{4}$$

$$\Delta K_c = K_c(n+1) - K_c(n) \tag{5}$$

For this study the Eq. (3) is applied to all hourly K_c measurements over the day to calculate the hourly intraday variability.

3.3. Variability Index

To estimate the daily variability corresponding to a given day we will use the variability index proposed in [16]. The variability index VI (Eq. 5) for a period of time is defined as the ratio between the length L of the sequence of line segments connecting the points of the GHI time series in W/m^2 and the length L_{cs} of the sequence of line segments connecting the points of the GHI_{clear} time series over a given period of time.

$$VI = \frac{\sum_{n=2}^{N} GHI(n) - GHI(n-1) + \Delta t^2}{\sum_{n=2}^{N} GHI_{clear}(n) - GHI_{clear}(n-1) + \Delta t^2}, \tag{6}$$

where Δt is the time step between two consecutive GHI (or GHI_{clear}) values.

An example of the line length calculated for both clear and cloudy days for one minute irradiance data is shown in Fig. 2. It can be seen that any measured GHI variability will increase the length of GHI relative to the clear sky model line.

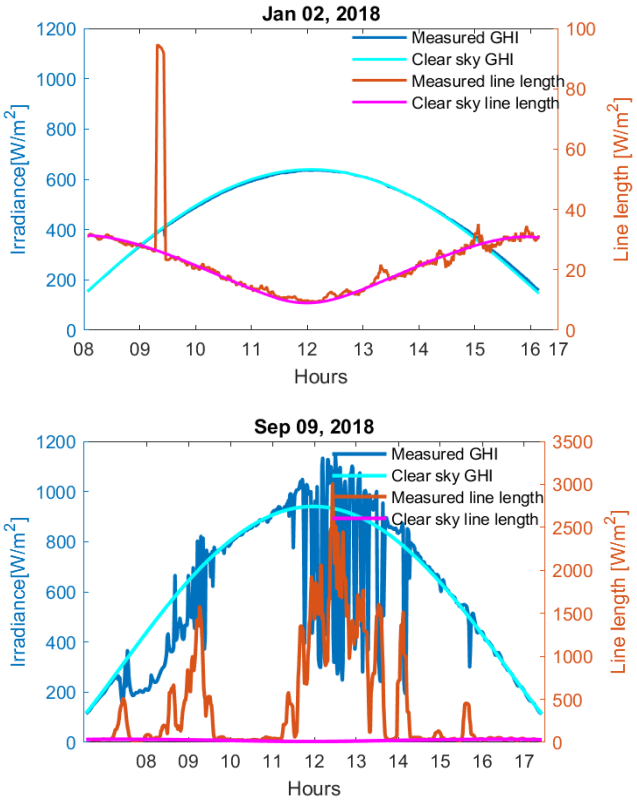

Fig. 2. Line length of GHI (W/m^2) on a clear day (top) and a cloudy day in (bottom). Blue line: GHI, Cyan line: GHI_{clear}, magenta line: measured line length L, Brown line: clear sky line length L_{cs}

In our case, the variability index is calculated by using the Eq. (4). For a given day, we will consider the difference between the hourly value of GHI and GHI_{clear} throughout the day considered, and the Δt is 1 hour.

3.4. Sunshine Number

The sunshine number SSN (t) is defined as a binary random variable depending on time [14].

$$SNN(t) = \begin{cases} 0 \text{ if the sun is covered by clouds at time t} \\ 1 \text{ otherwise} \end{cases} \tag{7}$$

The SSN value series are derived from irradiance values using the sunshine criterion [27]: "The sun shines" at time t if it is direct solar irradiation exceeds 120 Wm^2.

$$SNN(t) = \begin{cases} 1 & \text{if} \quad DNI > 120\ W/m^2 \\ 0 & \text{otherwise} \end{cases} \tag{8}$$

Fig. 3 illustrates an example of SSN representation. We have represented both clear and unclear day types. For Jan 01, 2018, which is a clear day from sunrise to sunset with VI =1, we can see that SSN is equal to 1 all day with a percentage of sunny moments equal to 100%. For Feb 05, 2018, which is a variable day VI=21, we can notice that for the first half of the day until noon the sky is clear and the SSN=1 while for the afternoon the radiance is very variable and we can observe a variation of SSN between 0 and 1

during this day the totality of the sunny moments is 46% and of the overcast moments 54%.

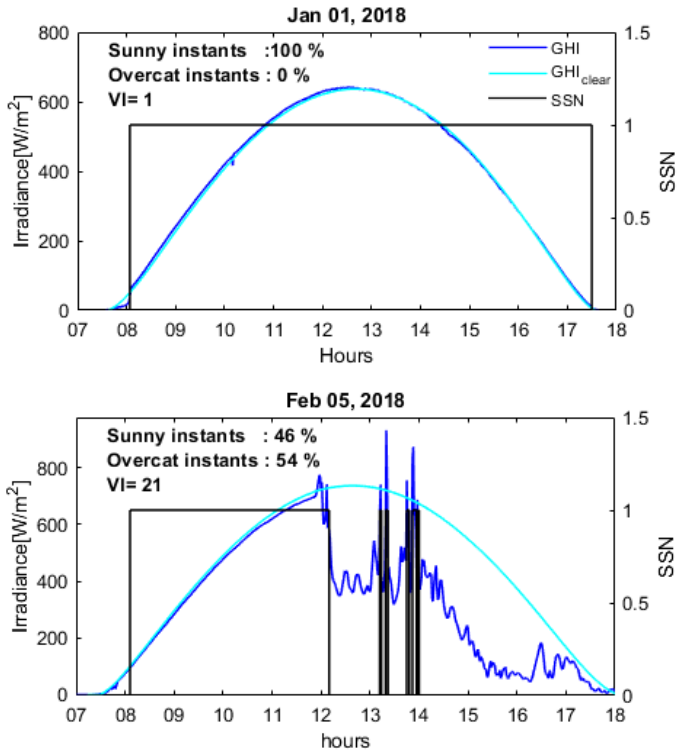

Fig. 3. The variation of solar irradiance GHI, sunshine number (black line), and GHI_{clear} as reference (cyan line).

4. Results

4.1. Seasonal Variability in Solar Irradiance

The seasonal variability of solar irradiance is caused by clouds, as well as by the daily and seasonal solar cycle. The daily solar cycle is in charge of the parabolic form of the solar irradiance: the irradiance increases after sunrise until solar noon and decreases until sunset. The seasonal solar cycle is also responsible for the change in radiation values from one season to the next. Seasonal variability is clearly observed in the variation of the monthly mean solar irradiance (Fig. 4).

The seasonal variability of solar irradiance is caused by clouds, as well as by the daily and seasonal solar cycle. The daily solar cycle is in charge of the parabolic form of the solar irradiance: the irradiance increases after sunrise until solar noon and decreases until sunset. And the seasonal solar cycle is responsible for the change in radiation values from one season to the next. Seasonal variability is clearly observed in the variation of the monthly mean solar irradiance (Fig. 4).

Fig. 4 shows that the highest monthly averages for the GHI and GHI_{clear} are found in May, June, July, and August, with values ranging from 275 W/m^2 to 333 W/m^2 for the GHI and from 343 W/m^2 to 359 W/m^2 for the GHI clear. The lowest irradiance values are observed during November and December with GHI values of 142 W/m^2 and GHI_{clear} of 177

W/m^2 and 157 W/m^2 in November and December respectively. The observed differences between the monthly average of GHI_{clear} and GHI are due to the diffusion and absorption by clouds with always including the seasonal and daily solar cycle.

The variability is also observed for the DHI end BHI. It can be seen that for each month, the monthly average of BHI is higher than the monthly average of DHI, which indicates that for all months, clear sky conditions dominate cloudy conditions. For the months with prevailing clear conditions, the contribution of BHI is higher than that of DHI.

Fig. 4 shows that the highest monthly averages for the GHI and GHI_{clear} are found in May, June, July, and August, with values ranging from 275 W/m^2 to 333 W/m^2 for the GHI and from 343 W/m^2 to 359 W/m^2 for the GHI_{clear} The lowest irradiance values are observed during November and December with GHI values of 142 W/m^2 and GHI_{clear} of 177 W/m^2 and 157 W/m^2 for November and December respectively. The observed differences between the monthly average of the GHI_{clear} and the GHI are due to the diffusion and absorption by clouds with always including the seasonal and daily solar cycle.

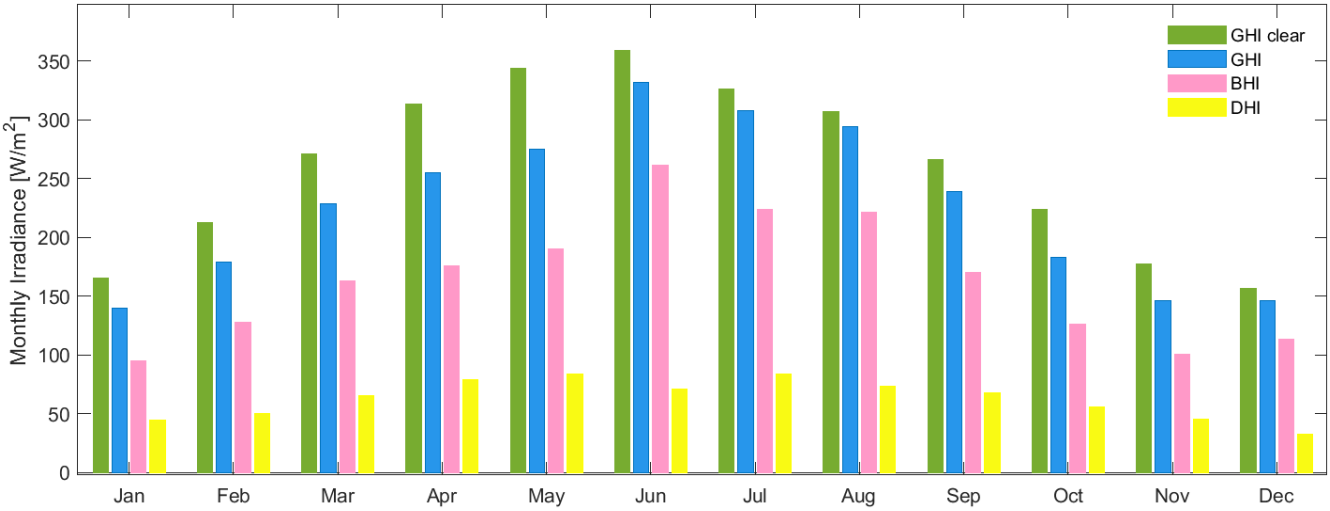

Fig. 4. The monthly mean of the GHIclear, GHI, BHI and DHI for the Benguerir site during 2018.

Since we are concerned to quantify the variability caused by clouds, the clear sky index is largely used in the literature to separate out the effects of clouds on the seasonal variability of solar irradiation. Then, to eliminate the seasonal and daily solar cycle, we will consider the variability of the clear sky index, which represents only the variability caused by the cloud.

4.2. Solar Irradiance Classification

The classification method used in this study extends to other studies [16], [28]. The classification is based on two statistics: the daily mean clear sky index K_c, and the intraday variability of clear sky index $\delta(K_c)$. The classification scheme delimits a two-dimensional space to group classes of solar irradiation by presenting the time series of the daily clear sky index as a function of the intraday variability, these classes of variability are also indicators of the state of the clouds. The classification space is unscrewed into nine classes in which the mean clear sky index is divided into three classes: overcast sky, mixed sky, and clear sky. The variability is divided into three categories: low, medium, and high variability.

Boundaries for each class were proposed by [28]. In our study, we have proposed other limits corresponding to the data used and adapting to the climate of the study region which is a semi-arid climate (BSh) according to Köppen Geiger climate classification [29].

To quantify the variability of solar irradiation caused by clouds, we grouped the clouds conditions and quantified the variability of solar irradiation according to our proposed boundaries. Fig. 5 shows the classification scheme with nine classes of cloud conditions for the data from 2018/01/01 to 2018/12/31. The x-axis shows the daily mean of the hourly clear-sky index and is divided into three classes: clear sky (A), mixed sky (B), and overcast sky (C). The y-axis shows the daily nominal variability and is divided into three classes: low variability (I), medium variability (II), and high variability (III). The nuances of gray indicate the probability density of daily variability. The pink, the green, and the blue correspond to the daily clear sky index for clear, mixed and overcast conditions respectively.

Fig. 5 displays the dispersion of the data corresponding to each class. Fig. 6 shows the percentage of data for each class on a daily basis. As illustrated in the figures, clear sky conditions with low variability are the most frequent with a percentage of 35.9%. Clear sky conditions with medium variability and mixed sky conditions with medium variability present 18.27% and 19.23% of the days respectively. Other classes are also present with low intensity ranging from 2.5% to 0.95%.

Fig. 7 shows an example of one-minute average irradiation for days corresponding to each class for the study site. The clear sky irradiation is shown in cyan for reference.

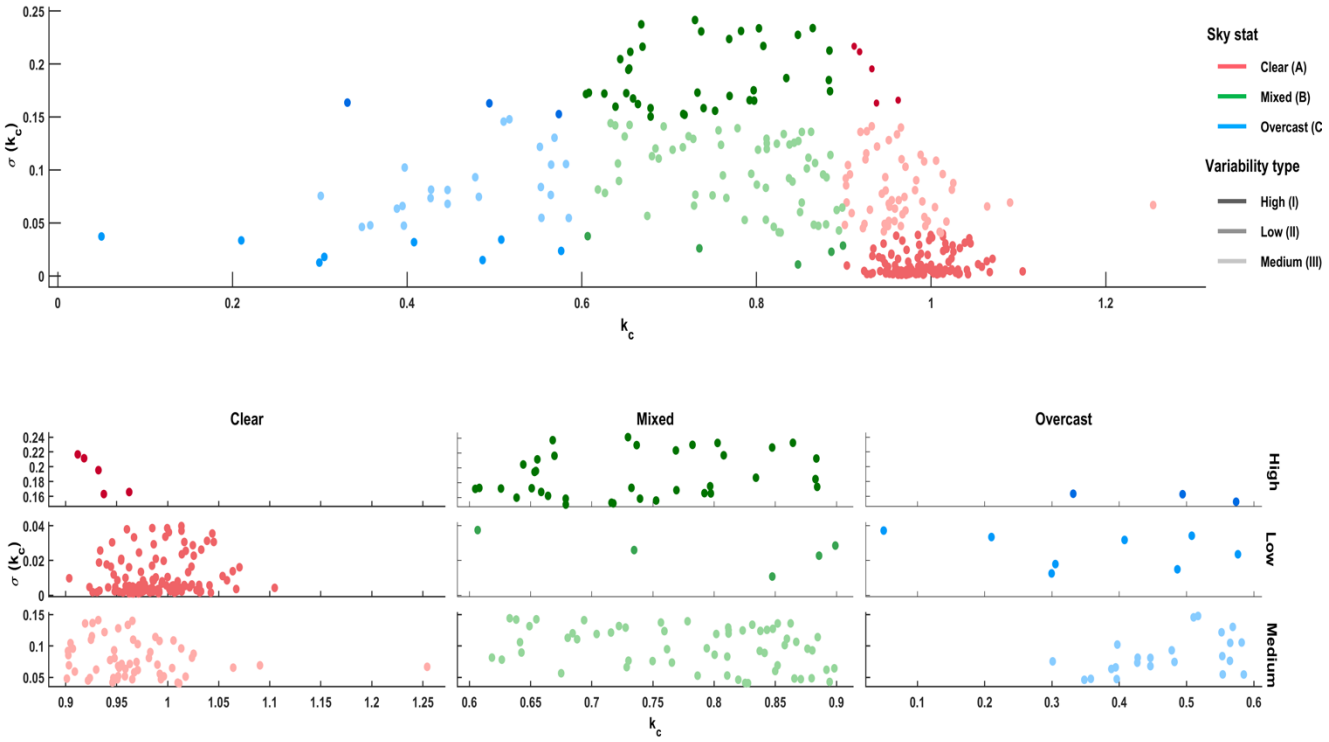

Fig. 5. The clouds classification in the two-dimensional space K_c-δ (K_c), bottom: the nine classes AI, AII, and AIII. BI, BII, BIII, and CI, CII, CIII.

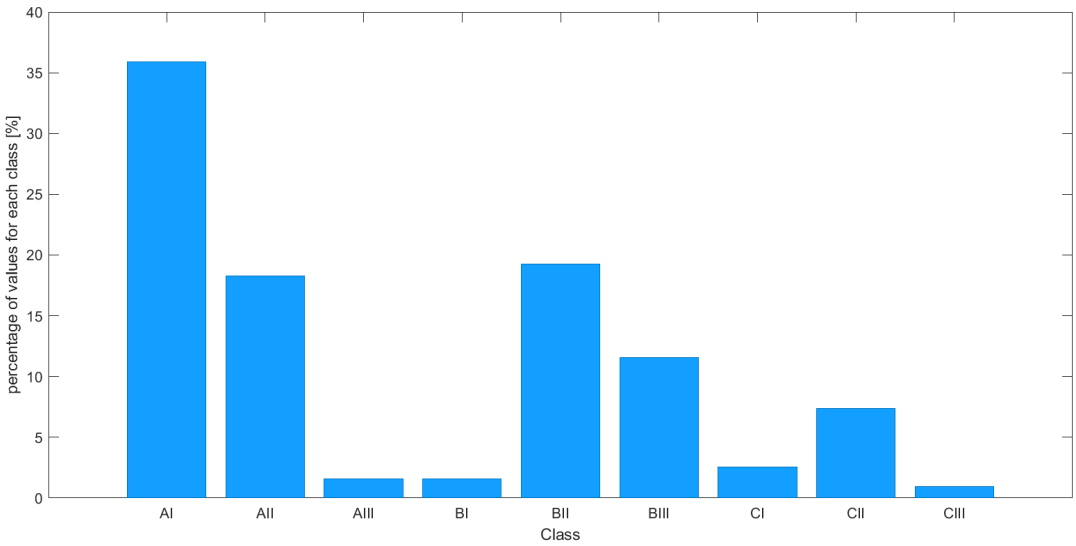

Fig. 6. The classification results in (%) for each class.

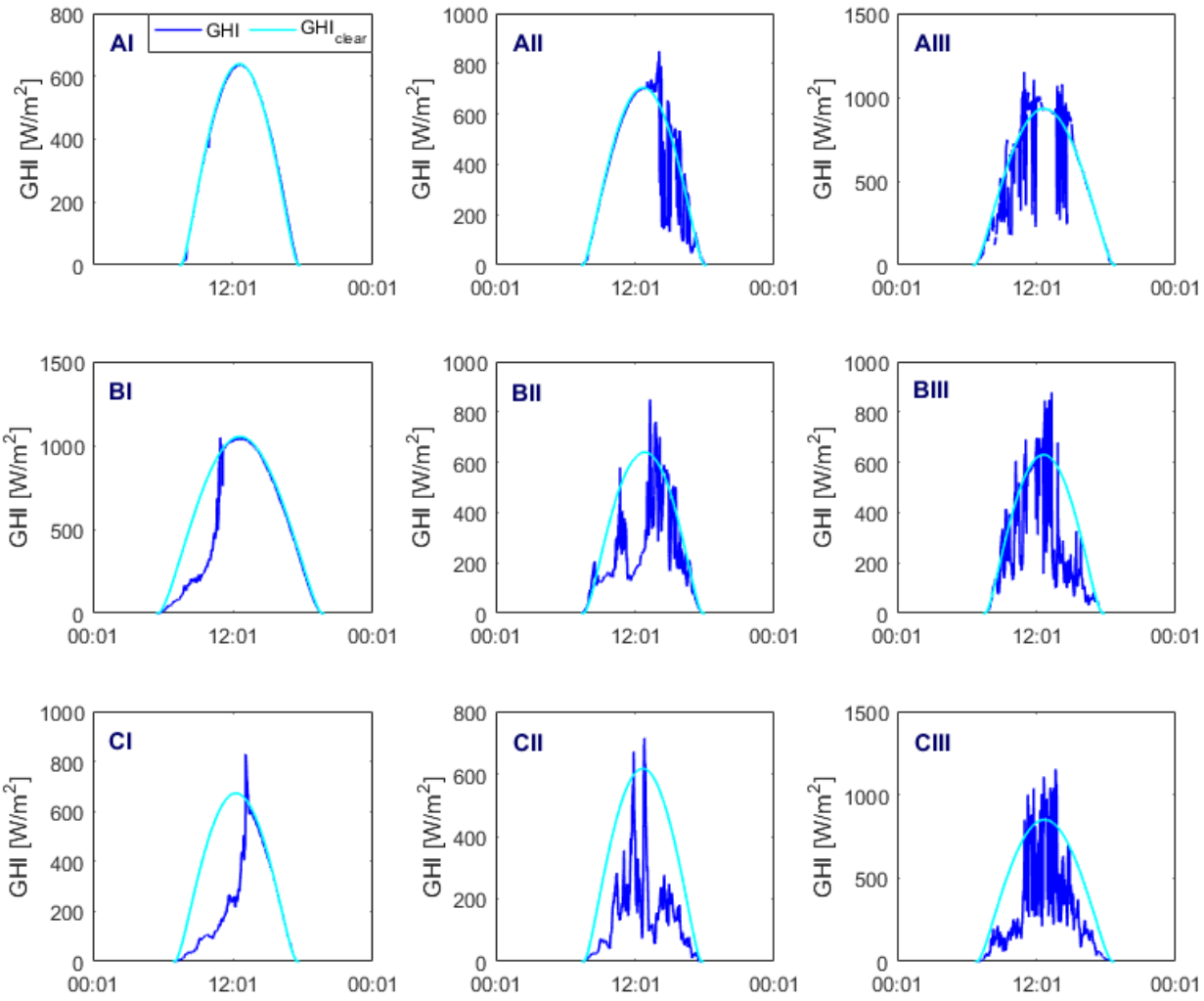

Fig. 7. Examples of a daily profile of the global irradiance corresponding to each class. The clear sky irradiance is indicated in cyan

4.3. Diffuse and Direct Components of Solar Irradiance per Cloud Condition

Changing clouds conditions also affects the other components of solar irradiance. To provide a general quantification, we have plotted the corresponding DHI and BHI averages for each class (Fig. 7). The BHI presents the solar irradiance coming directly from the solar disc, which means that clouds only have a blocking effect on the BHI. It can be observed that the highest value of the BHI is obtained for the CI class (192 W/m^2), and the lowest is obtained for the CII class with a value of 30 W/m^2. For the whole set of days, the BHI value decreases from clear to cloudy sky conditions.

For DHI it is observed that the value decreases from high variability to low variability with the lowest value of DHI is achieved for class A1 (55 W/m^2) and the high value for the BI (103.5 W/m^2). Clouds also scatter solar irradiance. For this reason, the DHI is higher for classes B and C.

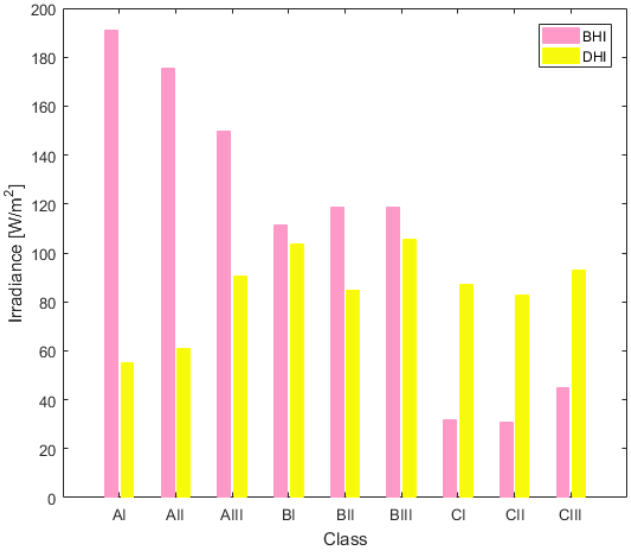

Fig. 8. The means of the DHI and BHI per class of the classification scheme.

4.4. Variability Index Performance

Several studies have used the variability index VI (Eq. (5)) for the classification of days. Fig. 9 shows the variability index obtained for the same days classified according to the variability of clear sky index and the clear sky index. It can be observed that on a clear day, VI is equal to 1, since the sum of the absolute values of the variations in irradiance would be equal to the same sum of the variations in clear sky irradiance. The high values of the variability index are obtained for days with highly variable irradiance. With the use of VI only for classification, we have noticed that low values of VI can be obtained in addition to clear days, for very cloudy or rainy days. Then a cloudy day and a clear day can have the same variability index. As observed in the figure, for the 8th day, the sky is mixed since it has a low variability index, and based only on this index for the classification this day could be considered as a clear day when it is not the case. This proves one of the limitations of the variability index: it cannot distinguish well between cloudy and clear. So, the use of the variability index only for the irradiation classification is insufficient, and in order to have good results, it is necessary to combine it with an additional quantity, which is the daily clearness index, to achieve an exact classification according to variability and cloud cover.

5. Summary and Conclusion

In this study, we quantify the temporal variability of solar irradiance caused by clouds. The classification was obtained by using two quantifiers: the daily mean of the clear sky index and the intraday variability. Nine classes are obtained according to different clouds conditions and variability types. The quantification of solar irradiance variability for our study site concludes that clear sky conditions with low variability are the most frequent conditions with a percentage of (38%). Clear and mixed sky with medium variability are also occurring, which can cause issues for power grid operators when integrating the energy produced from these two classes in terms of short-term fluctuations, for example. The classification system presented in this study can be useful for future studies to reduce the uncertainty in solar irradiation predictions, which is key to better integration of photovoltaic energy into power grids. In addition to the impact of the variability in the global irradiance, we also quantified the effect of this variability on the other components of radiation such as DHI and BHI. Finally, we established a comparison between the classification method based on the variability of clear sky index $\delta(K_c)$ and clear sky index K_c , and the variability index VI defined as the ratio between the length of the solar radiation time series and the length of the clear sky time series.

As a summary, the different quantifiers are summarized in Table 2 for January, 2018, the blue is used for clear sky, low variability and high sunshine, the pink for the mixed sky, medium variability, and medium sunshine, the orange for the unclear sky, high variability, and low sunshine. This type of matrix is useful to determine which metrology is more dominant than the others, as for example the first four days are classified as clear with low variability and high sunshine, the 18th day is characterized by an overcast sky, low variability, and medium sunshine.

Finally, it should be noticed that the different classes of our classification system represent the cloud conditions based on the time series of the clear sky index and not the physical properties of the clouds per class. In upcoming studies, we will be able to deepen our classification to obtain cloud-type by using hemispherical sky cameras. The classification method presented in this study can be used by future studies to reduce the uncertainty in solar irradiance predictions and allow accurate predictions, in order to allow efficient use of the fluctuating energy production of photovoltaic (PV) systems.

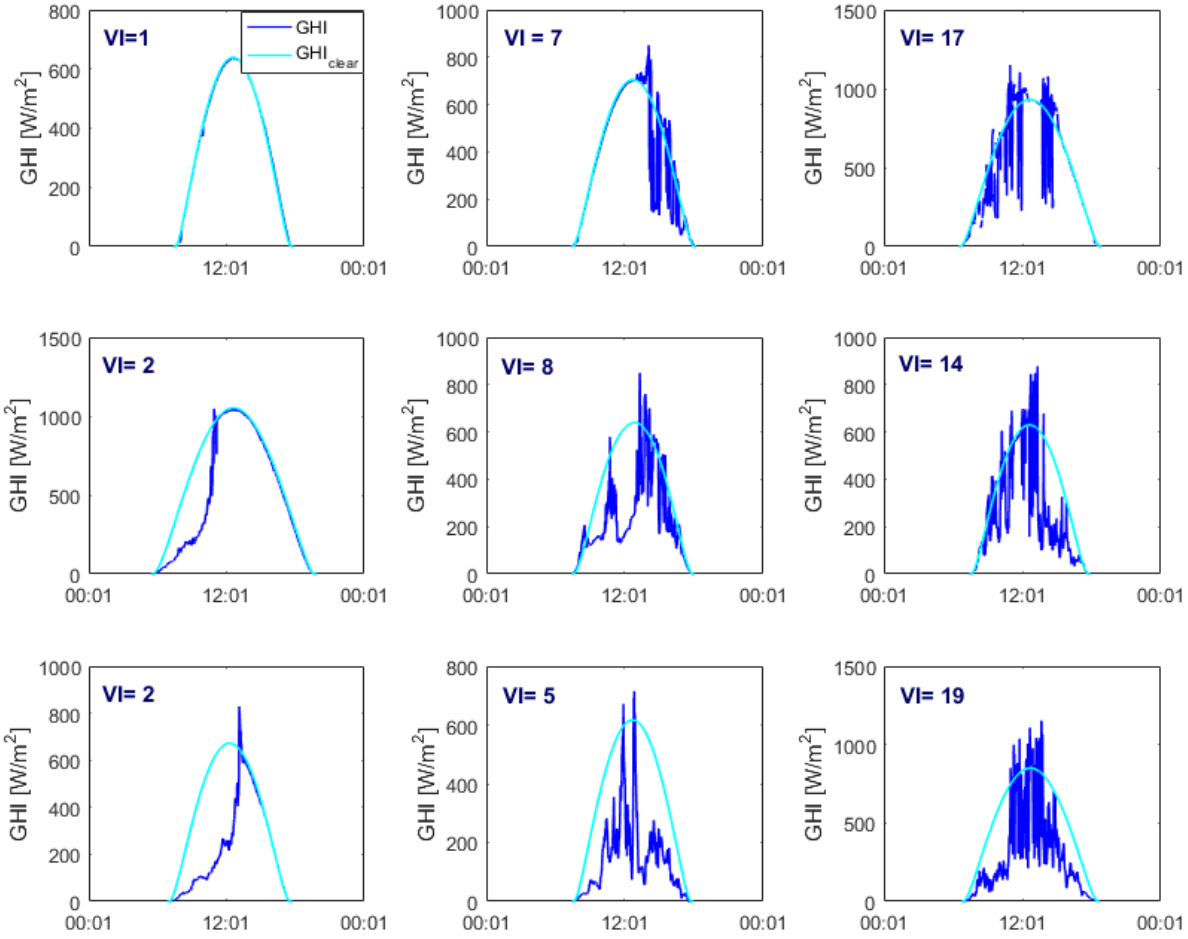

Fig. 9. Examples of days with increasing Variability Index VI values. The clear sky irradiance is indicated in cyan**.**

.

Table 2. Classification of days using the three quantifiers individually K_c, δ (K_c), and SSN for January, 2018 as an example.

	Clear sky, low variability, high sunshine					Mixed sky, medium variability, medium sunshine							Overcast, high variability low sunshine			
Day of month	1	2	3	4	5	6	7	8	9	10	11	12	13	14	15	16
variability																
Sky clarity																
SSN																
Day of month	17	18	19	20	21	22	23	24	25	26	27	28	29	30	31	
variability																
Sky clarity																
SSN																

ACKNOWLEDGMENT

The authors thank the Green Energy Park (GEP) and the Research İnstitute For Solar Energy and New Energies (IRESEN) for providing the solar radiation measurements.

References

1. S. Sobri, S. Koohi-Kamali, and N. A. Rahim, Solar photovoltaic generation forecasting methods: "A review, Energy Conversion and Management", vol. 156, pp. 459–497, 2018.
2. M. Yesilbudak, M. Çolak, and R. Bayindir. (2016, November). "A review of data mining and solar power prediction", In 2016 IEEE International Confe rence on Renewable Energy Research and Applications (ICRERA) (pp. 1117-1121). IEEE..
3. E. Taibi, T. Nikolakakis, L.Gutierrez, C.Fernandez, J. Kiviluoma, S.Rissanen, and T. J. Lindroos, 2018. "Power system flexibility for the energy transition: Part 1", Overview for policy makers. 2018.
4. A. M. Ismail, R. Ramirez-Iniguez, M. Asif, A. B. Munir, and F. Muhammad-Sukki. (2015). "Progress of solar photovoltaic in ASEAN countries: A review", Renewable and Sustainable Energy Reviews, 48, 399-412.
5. N. Lewis and D. Nocera. (2017). Market Report Series: Renewables 2017. J. Qual. Particip, 104(42), 20142-20142.
6. M. Colak, M. Yesilbudak, and R. Bayindir. (2019, November). "Forecasting of Daily Total Horizontal Solar Radiation Using Grey Wolf Optimizer and Multilayer Perceptron Algorithms", In 2019 8th International Conference on Renewable Energy Research and Applications (ICRERA) (pp. 939-942). IEEE.
7. A. K. Pani and N. Nayak. "Forecasting solar irradiance with weather classification and chaotic gravitational search algorithm based wavelet kernel extreme learning machine", International Journal of Renewable Energy Research (IJRER), 2019, vol. 9, no 4, p. 1650-1659.
8. M. Schroedter-Homscheidt, M. Kosmale, S. Jung, and J. Kleissl, "Classifying ground-measured 1 minute temporal variability within hourly intervals for direct normal irradiances", Meteorologische Zeitschrift, vol. 27, no. 2, pp. 161–179, 2018.
9. A. Alzahrani, P. Shamsi, M. Ferdowsi, and C. Dagli. (2017, November). "Solar irradiance forecasting using deep recurrent neural networks", In 2017 IEEE 6th international conference on renewable energy research and applications (ICRERA) (pp. 988-994). IEEE..
10. M. Lave, M. J. Reno, and R. J. Broderick. (2015). "Characterizing local high-frequency solar variability and its impact to distribution studies", Solar Energy, 118, 327-337.
11. T. Takamatsu and T. Y. Nakajima. (2018, October). "Study of Spatial Asynchrony Analysis for Solar Irradiance", In 2018 7th International Conference on Renewable Energy Research and Applications (ICRERA) (pp. 711-714). IEEE.
12. M. Omar, A. Dolara, G. Magistrati, M. Mussetta, E. Ogliari, and F. Viola. (2016, November). "Day-ahead forecasting for photovoltaic power using artificial neural networks ensembles", In 2016 IEEE International Conference on Renewable Energy Research and Applications (ICRERA) (pp. 1152-1157). IEEE.
13. R. Blaga, A. Sabadus, N. Stefu, C. Dughir, M. Paulescu, and V. Badescu. (2019), "A current perspective on the accuracy of incoming solar energy forecasting", Progress in Energy and Combustion Science, 70, 119-144.
14. V. Badescu and M. Paulescu. (2011). "Statistical properties of the sunshine number illustrated with measurements from Timisoara (Romania) ", Atmospheric research, 101(1-2), 194-204.
15. R. Perez, S. Kivalov, J. Schlemmer, K. Hemker Jr, and T. E. Hoff. (2012). "Short-term irradiance variability: Preliminary estimation of station pair correlation as a function of distance", Solar Energy, 86(8), 2170-2176.
16. J. Stein, C. Hansen, and M. J. Reno. (2012). The variability index: A new and novel metric for quantifying irradiance and PV output variability (No. SAND2012-2088C). Sandia National Laboratories.
17. B. O. Kang and K.-S. Tam. (2013). "A new characterization and classification method for daily sky conditions based on ground-based solar irradiance measurement data", Solar Energy, 94, 102-118.
18. P. Lauret, R. Perez, L. M. Aguiar, E. Tapachès, H. M. Diagne, and M. David. (2016). "Characterization of the intraday variability regime of solar irradiation of climatically distinct locations", Solar Energy, 125, 99-110.
19. R. Blaga and M. Paulescu. (2018). "Quantifiers for the solar irradiance variability: A new perspective", Solar Energy, 174, 606-616.
20. G. M. Lohmann. (2018). "Irradiance variability quantification and small-scale averaging in space and time: A short review", Atmosphere, 9(7), 264.
21. A. T. Fernandes, L. F. Lourenço, R. M. Monaro, and J. R. Cardoso. (2019, November). "Statistical Modeling of Solar Irradiance for Northeast Brazil", In 2019 8th International Conference on Renewable Energy Research and Applications (ICRERA) (pp. 386-391). IEEE.
22. X. Sun, J. M. Bright, C. A. Gueymard, B. Acord, P. Wang, and N. A. (2019). "Worldwide performance assessment of 75 global clear-sky irradiance models using principal component analysis", Renewable and Sustainable Energy Reviews, 111, 550-570.
23. M. Lefèvre, A. Oumbe, P. Blanc., B. Espinar, B. Gschwind, Z. Qu, L. Wald, M. Homscheidt, C. Hoyer-Klick, A. Arola, A. Benedetti, J. Kaiser, and J. Morcrette (2013). "McClear: a new model estimating downwelling solar radiation at ground level in clear-sky conditions", Atmospheric Measurement Techniques, 6, 2403-2418.

24. M. Schroedter-Homscheidt, A. Arola, N. Killius, M. Lefèvre, L. Saboret, W. Wandji, L. Wald, and E. Wey. (2016, October). The Copernicus atmosphere service (CAMS) radiation service in a nutshell. (2016, October)

25. O. E. Alani, A. Ghennioui, A. A. Merrouni, H. Ghennioui, Y.-M. Saint-Drenan, and P. Blanc. (2019, July). "Validation of surface solar irradiances estimates and forecast under clear-sky conditions from the CAMS McClear model in Benguerir, Morocco", In AIP Conference Proceedings (Vol. 2126, No. 1, p. 190005). AIP Publishing LLC.

26. C. F. Coimbra, J. Kleissl, and R. Marquez. (2013). "Overview of solar-forecasting methods and a metric for accuracy evaluation", Solar energy forecasting and resource assessment, 171-194.

27. 'World Meteorological Organization', World Meteorological Organization. [Online]. Available: https://public.wmo.int/en. [Accessed: 31-Aug-2020]

28. L. M. Aguiar, B. Pereira, M. David, F. Díaz, and P. Lauret. (2015). "Use of satellite data to improve solar radiation forecasting with Bayesian Artificial Neural Networks", Solar Energy, 122, 1309-1324.

29. J. Ascencio-Vásquez, K. Brecl, and M. Topič. (2019). "Methodology of Köppen-Geiger-Photovoltaic climate classification and implications to worldwide mapping of PV system performance", Solar Energy, 191, 672-685.

30.